Dynamic Response of Vertically Loaded Nonlinear Pile Foundations

By Toyoaki Nogami,[1] M. ASCE, and Kazuo Konagai[2]

Abstract: Nonlinear conditions are implemented in the time domain formulation for the dynamic response of pile foundations previously developed by the writers. Both single and group piles subjected to vertical dynamic load are considered. In the present study, the nonlinear effects in the vertical response are assumed to result from slippage of the pile from the soil. In order to demonstrate the capability of the present formulations and to see the effects of nonlinearity on the dynamic response of pile foundations, pile foundation responses are computed for both harmonic and transient load. Various interesting observations are made based upon the computed results.

Introduction

The dynamic response of pile foundations has been formulated by various researchers. The frequency domain finite element method was used for both single piles (2,6,7) and group piles (22) under linear elastic conditions. The frequency domain finite method was further used for nonlinear pile foundations but limited to single piles (1). To account for the nonlinearity, the soil constitutive relationship proposed by Hardin and Drnevich (3) was implemented in the finite element method.

Solving wave equations for the normal modes of the soil stratum, analytical expressions for the frequency domain soil response were obtained and used for the frequency domain dynamic response analysis of linear elastic single piles (8,9,19) and pile groups (10). Wave equations were also solved to obtain the expression for the frequency domain soil response due to a circular ring load, and the dynamic response of linear elastic piles was formulated in the frequency domain for both single and group piles (5,21).

In order to simplify the solution and economize the computation, a Winkler's hypothesis was used to formulate the frequency domain response of linear elastic single piles (18) and pile groups (11,13,14,20). In this approach, the analytical expressions for the soil response were obtained by solving wave equations applied to a plane strain medium. This approach based on a Winkler's hypothesis was further applied to the nonlinear single pile response analysis in the frequency domain (15), in which the cyclic unit load transfer curves, widely used in the "static" cyclic response analysis of piles, were used together with the expression for the soil response developed in Ref. 18.

Following a Winkler's hypothesis, the time domain expression for the dynamic response of single and group piles were developed for piles

[1]Assoc. Head of Ocean Engrg., Scripps Inst. of Oceanography, Univ. of California, San Diego, CA 92093.

[2]Assoc. Prof., Dept. of Civ. Engrg., Technological Univ. of Nagaoka, Nagaoka, Japan.

Note.—Discussion open until July 1, 1987. To extend the closing date one month, a written request must be filed with the ASCE Manager of Journals. The manuscript for this paper was submitted for review and possible publication on February 10, 1986. This paper is part of the *Journal of Geotechnical Engineering*, Vol. 113, No. 2, February, 1987. ©ASCE, ISSN 0733-9410/87/0002-0147/$01.00. Paper No. 21252.

subjected to dynamic axial load (5,17). The time domain Winkler soil model in this expression was developed by solving wave equations applied to a plane strain medium. However, the conditions considered are lmited to linear elastic conditions, which may not be realistic for predicting the behavior of highly nonlinear systems such as pile foundations. The present study extends the previous studies made for the time domain analysis of linear pile foundations (5,17) and considers the nonlinear conditions.

FORMULATIONS

Following a Winkler's hypothesis, the soil reaction force to the pile shaft is assumed to be related to the soil response only at the depth where the reaction force is considered. Visual presentation of this idealization is given in Fig. 1. In addition, the behavior of the soil at a given depth is assumed to be that of an elastic plane strain continuous medium. All of those assumptions have been examined and found to be reasonable (12,13,14). It has been observed that the nonlinearity in the vertical response of the axially loaded pile is mainly due to slippage at the soil-pile interface. Thus, the present formulation considers slippage at the soil-pile interface.

Soil-Response.—A massless rigid disk is assumed to be embedded in a plane strain medium (Fig. 2). The steady-state response of the medium for a harmonic load applied to the disk is approximately expressed as (5,17)

$$w(a_0, r) = \sqrt{\frac{r_0}{r}} \sum_{n=1}^{3} \frac{1}{k_n + ic_n a_0} e^{-ia_0(r-r_0)/r_0} p(a_0) \quad (1)$$

where r_0 = radius of the disk; $a_0 = r_0\omega/v_s$; ω = circular frequency; v_s = shear wave velocity; r = distance measured from the center of the disk;

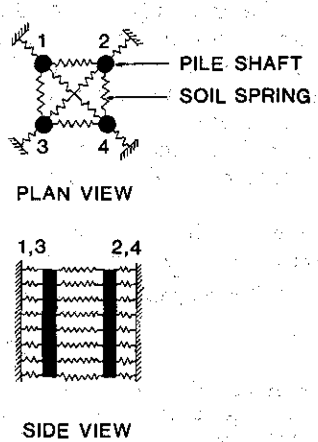

FIG. 1.—Schematic View of Winkler Idealization

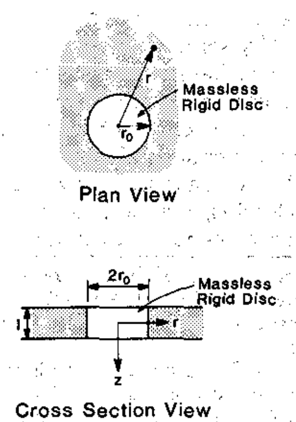

FIG. 2.—Massless Rigid Disk Embedded in Plane Strain Medium

$w(a_0, r)$ = vertical displacement amplitude of the medium; and $p(a_0)$ = amplitude of the force. Denoting G_s as a shear modulus of the medium, k_n and c_n are given as

$$\frac{1}{G_s} k_1 = \begin{cases} 3.518 \left(\frac{r_0}{r}\right)^{0.624} & 1 \le \frac{r}{r_0} \le 40 \\ 0.352 & 40 \le \frac{r}{r_0} \end{cases} \quad \text{(2a)}$$

$$\frac{1}{G_s} k_2 = \begin{cases} 3.518 \left(\frac{r_0}{r}\right)^{0.359} & 1 \le \frac{r}{r_0} \le 28.6 \\ 1.074 & 28.6 \le \frac{r}{r_0} \end{cases} \quad \text{(2b)}$$

$$\frac{1}{G_s} k_3 = \begin{cases} 5.529 \left(\frac{r_0}{r}\right)^{0.162} & 1 \le \frac{r}{r_0} \le 5.4 \\ 4.202 & 5.4 \le \frac{r}{r_0} \end{cases} \quad \text{(2c)}$$

$$\frac{v_s}{G_s r_0} \begin{Bmatrix} c_1 \\ c_2 \\ c_3 \end{Bmatrix} = \begin{cases} 113.097 \\ 25.133 & r \ge r_0 \\ 9.362 \end{cases} \quad \text{(2d)}$$

The preceding approximate expression for the soil response is obtained by using three Voigt models connected in series to reproduce the soil behavior at the pile shaft ($r = r_0$) and by implementing the characteristics of the cylindrical shear wave propagation.

Applying an inverse Fourier transformation to Eq. 1, the response of the medium due to the trapezoidal load shown in Fig. 3 is expressed in the time domain as (5,17)

$$w(t, r) = p(0) \sum_{n=1}^{3} H_n(t, r) + p(\Delta t) \sum_{n=1}^{3} I_n(t, r) \quad \text{(3)}$$

in which t = time; Δt = duration of trapezoidal load applied; and $p(0)$

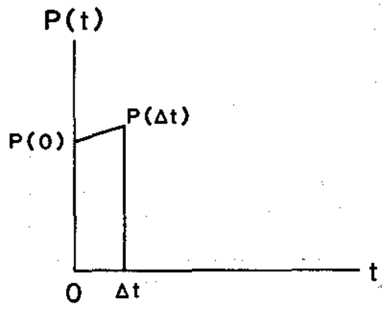

FIG. 3.—Trapezoidal Load Applied during Period *t*

and $p(\Delta t)$ = magnitudes of the trapezoidal load at $t = 0$ and Δt, respectively. Denoting $t_0 = (r - r_0)/v_s$ and $\kappa_n = k_n/c_n$, $H_n(t,r)$ and $I_n(t,r)$ are

$$t \geq t_0 \quad H_n(t,r) = \sqrt{\frac{r_0}{r}}\frac{1}{k_n}\left\{\frac{1}{\kappa_n\Delta t}e^{\kappa_n\Delta t} - \left(1 + \frac{1}{\kappa_n\Delta t}\right)\right\}e^{-\kappa_n(t-t_0)} \quad \text{(4a)}$$

$$\text{and} \quad I_n(t,r) = \sqrt{\frac{r_0}{r}}\frac{1}{k_n}\left\{\left(1 - \frac{1}{\kappa_n\Delta t}\right)e^{\kappa_n\Delta t} + \frac{1}{\kappa_n\Delta t}\right\}e^{-\kappa_n(t-t_0)} \quad \text{(4b)}$$

$$t < t_0 \quad H_n(t,r) = 0 \quad \text{and} \quad I_n(t,r) = 0 \quad \text{(4c)}$$

The time history of the soil reaction force is digitized at every time interval, Δt, and is assumed to be a piecewise linear variation with time as shown in Fig. 4. The soil response to the force shown in Fig. 4 can be expressed at time t_i from Eq. 3 as (5,17)

$$w(t_i, r) = \sum_{n=1}^{3} I_n(\Delta t, r)p(t_i) + \sum_{n=1}^{3} H_n(\Delta t, r)p(t_{i-1}) + \sum_{n=1}^{3} w_n(t_{i-1}, r)e^{-\kappa_n\Delta t} \quad (5)$$

When N piles in a group are considered, Δt is set to be less than $(r-r_0)/v_s$ to ensure that the wave induced in the soil at the piles does not reach other piles during the period Δt. Under this time interval Δt, Eq. 5 at the location of the lth pile becomes as

$$w(t_i) = \sum_{n=1}^{3} I_n(\Delta t, r_0)p(t_i) + \sum_{n=1}^{3} H_n(\Delta t, r_0)p(t_{i-1})$$

$$+ \sum_{n=1}^{3}\sum_{m=1}^{N} w_n(t_{i-1}, r_{lm})e^{-\kappa_n\Delta t} \quad (6)$$

in which $w(t_i)$ and $p(t_{i-1})$ = displacement and force at the locations of the lth pile, respectively; and r_{lm} = distance between the lth and mth piles. Thus, inverting Eq. 6, the soil reaction forces at the lth pile for a given depth are expressed as

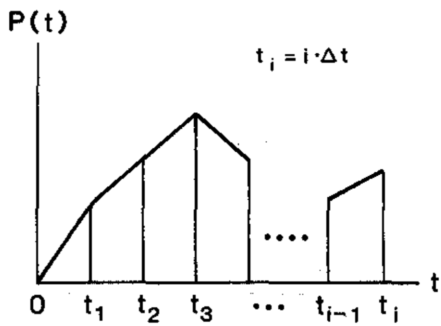

FIG. 4.—Piecewise Linear Time History

$$p_i = kw_i + d_i \quad (7)$$

in which $p_i = p(t_i)$ and $w_i = w(t_i)$; k and d_i are known at t_i and expressed as

$$k = \frac{1}{\sum_{n=1}^{3} I_n(\Delta t, r_0)} \quad (8a)$$

$$d_i = -kp(t_{i-1}) \sum_{n=1}^{3} H_n(\Delta t, r_0) - k \sum_{m=1}^{N} \sum_{n=1}^{3} w_n(t_{i-1}, r_{lm}) e^{-\kappa_n \Delta t} \quad (8b)$$

Similarly, the soil reactions for all other piles can be expressed by Eq. 7. This equation for each pile is independent of and not coupled with w_i at other piles. The effects of other piles appear through d_i which is a known value at $t = t_i$.

When the slippage between the soil and pile is allowed, Eq. 7 is modified to consider the slippage as

$$p_i = k(W_i - y_i) + d_i \quad (9)$$

in which y_i = cumulative slippage displacement; W_i = displacement of pile shaft; and $w_i = W_i - y_i$. The slippage starts when p_i reaches $2\pi r_0 \tau_f$, in which τ_f = the maximum shear stress allowed at the soil-pile interface, and stops when the velocity, $\dot{y}$, becomes zero. When slippage does not occur during the period from t_{i-1}–t_i, y_i is known and $= y_{i-1}$ in Eq. 9. On the other hand, when slippage does occur, p_i is known and $2\pi r_0 \tau_f$ but y_i is unknown in Eq. 9. Thus, during slippage, the unknown displacement, y_i, is governed by

$$2\pi r_0 \tau_f = k(W_i - y_i) + d_i \quad (10)$$

Pile Response.—The soil-pile system is divided into a number of horizontal slices as shown in Fig. 5. The response of a pile segment to the dynamic load is governed by

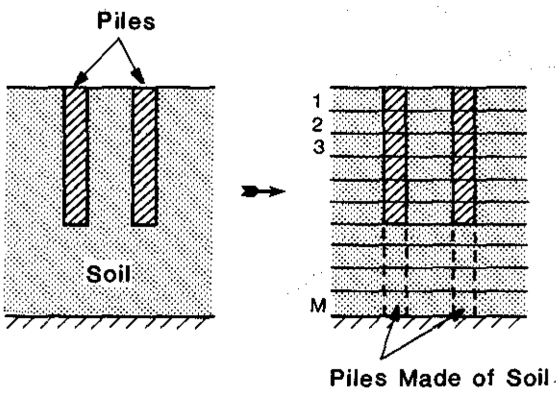

FIG. 5.—Soil-Pile System Divided into Horizontal Slices

$$E_pA\frac{d^2W_i}{dz^2} - p_i = m_p\ddot{W}_i \qquad (11)$$

in which E_pA = axial stiffness of the pile shaft; m^p = mass per unit length of the pile shaft; and p_i = soil reaction force to the pile ($p_i \leq 2\pi r_0\tau_f$). The soil reaction force, p_i, is

$$p_i = \begin{cases} k(W_i - y_{i-1}) + d_i & \text{(during no slippage)} \\ 2\pi r_0\tau_f & \text{(during slippage)} \end{cases} \qquad (12)$$

When the increment of the acceleration, $\ddot{W}$, is assumed to be proportional to t^α, the velocity and acceleration of the pile are related with the displacement, W_i, through

$$\dot{W}_i = \frac{\alpha+2}{\Delta t}w_i - \frac{\alpha+2}{\Delta t}W_{i-1} - (\alpha+1)\dot{W}_{i-1} - \frac{\alpha\Delta t}{2}\ddot{W}_{i-1} \qquad (13a)$$

$$\ddot{W}_i = \frac{(\alpha+1)(\alpha+2)}{\Delta t^2}W_i - \frac{(\alpha+1)(\alpha+2)}{\Delta t^2}W_{i-1} - \frac{(\alpha+1)(\alpha+2)}{\Delta t}\dot{W}_{i-1}$$

$$- \frac{(\alpha+1)(\alpha+2)}{2}\ddot{W}_{i-1} \qquad (13b)$$

in which α = a constant to control the solution stability in a numerical computation ($-1 < \alpha \leq 0$).

Substitution of Eqs. 12 and 13 into Eq. 11 results in

$$\frac{d^2W_i}{dz^2} - \lambda^2W_i = \gamma_i \qquad (14)$$

where during no slippage

$$\lambda^2 = \frac{m_p}{E_pA}\frac{(\alpha+1)(\alpha+2)}{\Delta t^2} + \frac{k}{E_pA} \qquad (15a)$$

$$\gamma_i = (d_i - ky_i) - \frac{m_p}{E_pA}\left\{\frac{(\alpha+1)(\alpha+2)}{\Delta t}W_{i-1} + \frac{(\alpha+1)(\alpha+2)}{\Delta t}\dot{W}_{i-1}\right.$$

$$\left. + \frac{(\alpha+1)(\alpha+2)}{2}\ddot{W}_{i-1}\right\} \qquad (15b)$$

and during slippage

$$2 = \frac{m_p}{E_pA}\frac{(\alpha+1)(\alpha+2)}{\Delta t^2} \qquad (16a)$$

$$r_i = 2\pi r_0\tau_f - \frac{m_p}{E_pA}\left\{\frac{(\alpha+1)(\alpha+2)}{\Delta t}W_{i-1} + \frac{(\alpha+1)(\alpha+2)}{\Delta t}\dot{W}_{i-1}\right.$$

$$\left. + \frac{(+1)(+2)}{2}\ddot{W}_{i-1}\right\} \qquad (16b)$$

The solution for Eq. 14 is given in Refs. 5 and 17. In the solution, the displacement of a segment is expressed as a polynominal function of z with the least number of terms, required to account for the boundary conditions at the upper and lower ends of the segment (four terms). The solution accounts for the layered nonhomogeneity of the soil medium.

Nonlinear Responses of Pile Foundations

Response to Harmonic Excitation.—Both a single pile and a group of piles in a homogeneous soil medium are considered. A group of piles is assumed to be attached to a common massless rigid cap. Rigid bedrock is assumed to be located either at the pile tip or at a depth as great as twice of the pile shaft length. Although various distributions of τ_f along the pile shaft can be considered, a simple linear variation from τ_f at the pile head to $2\tau_f$ at the pile tip is considered in the present study. Information of the soil and pile foundations is given in Fig. 6 further.

A harmonic load of amplitude, P, is applied at the pile head. Excitation frequency is given in terms of the frequency parameter a_0 ($=r_0\omega/v_s$) and is $a_0 = 0.3$. Fig. 7 shows the time history of the pile-head displacement of a single pile for various $P/(\tau_f L^2)$ ratios, in which L = the length of the pile shaft. It is noted that $P/(\tau_f L^2) = 0$ corresponds to the case in which slippage is not allowed in the analysis. Fig. 8 shows the time histories of the soil reaction force and of the cumulative soil slippage displacement at a depth near the ground surface. It is seen in the figures that the nonlinearity (slippage) increases the maximum pile-head displacement and changes the phase shift.

The time histories of the pile-head response were computed for harmonic excitation given at the head. The maximum response and phase shift were read in the time histories where the responses were in a steady state. With those values, the pile-head stiffnesses were computed for various frequencies. Fig. 9 shows the pile-head stiffnesses of single end-bearing and floating piles at various frequencies. When severe nonlinearity develops in end-bearing piles, the real part of the stiffness is reduced to the stiffness of a pile shaft alone and the imaginary part increases very little with frequency. When severe nonlinearity develops in floating piles, the real part of the stiffness is drastically reduced to a very small number and the imaginary part increases with frequency even faster than it does under elastic conditions. Thus, at high frequencies (say $a_0 > 0.4$), the nonlinear environment can significantly increases the damping effect in floating piles.

The stiffnesses of a 2×2 end-bearing pile group are shown in Fig. 10. It is of great interest that nonlinearity affects the group stiffness very significantly at the frequencies around the peaks, even when it does very little at very small frequencies. This is because the slippage length increases along the pile shaft at the frequencies around the peaks (Fig. 11) and thus the interaction effects are decreased. It is noted that the slippage depth shown in Fig. 11 is the greatest depth at which slippage occurs. However, slippage is not necessarily induced simultaneously all along the slippage depth shown in the figure.

Response to Transient Load.—A transient loading as shown Fig. 12 is applied at the head of single piles. The pile and soil considered in the

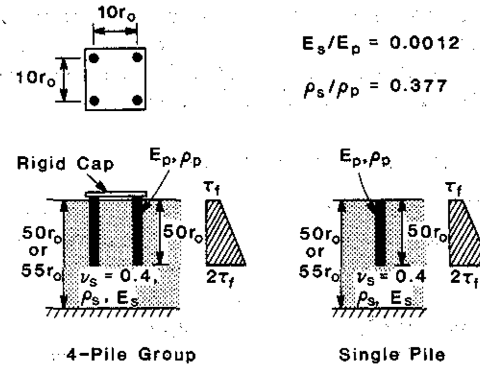

FIG. 6.—Pile Foundations Considered

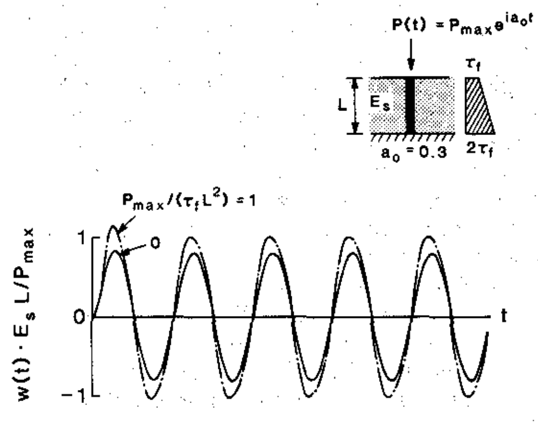

FIG. 7.—Time Histories of Pile-Head Displacement

analyses are identical to those shown in Fig. 6 but only single piles are considered.

The displacement time histories of the pile-head subjected to a transient load are shown in Fig. 13 for both end-bearing and floating piles. The difference between the responses of those two piles is remarkable as is seen in Fig. 13. The nonlinearity of the system increases the peaks in the transient response of end-bearing piles but produces very little permanent displacement. On the other hand, the amount of permanent displacement of floating piles is sensitive to the magnitude of the load applied and can be very significant. Because of a very high damping as observed for floating piles subjected to harmonic motion, floating piles do not oscillate.

The slippage at the soil-pile interface causes a permanent relative displacement between the soil and pile. This results in a residual skin friction along the side of the pile and residual axial force in the pile shaft. Fig. 14 shows those forces after the transient load is applied. The residual forces are more significant for a floating pile than for an end-bearing

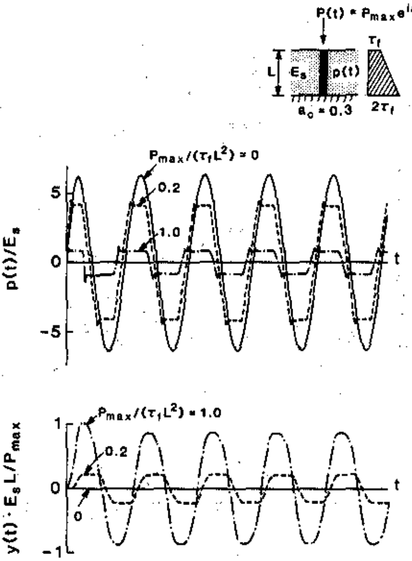

FIG. 8.—Time Histories of Skin Friction and Cumulative Slippage Displacement at Soil-Pile Interface near Ground Surface

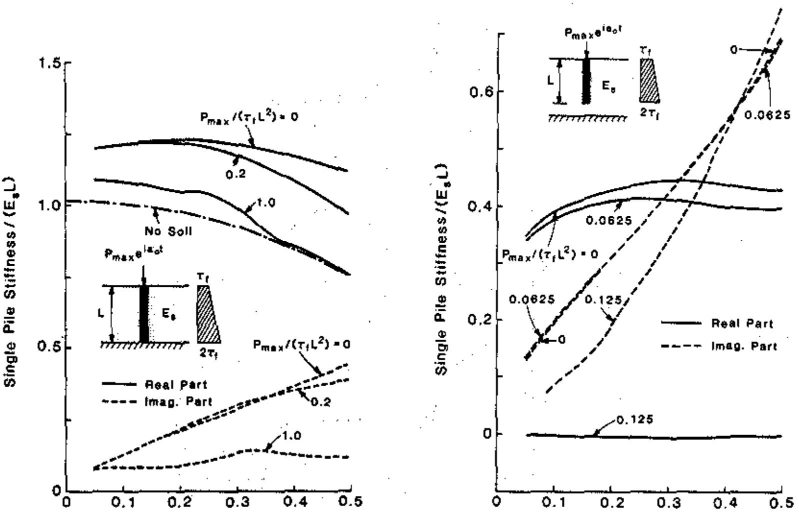

FIG. 9.—Pile-Head Stiffness of Single Pile: (*a*) End-Bearing Pile; (*b*) Floating Pile

pile. The interesting features observed in the residual forces in a floating pile are as follows:

1. The distribution pattern along the pile shaft depends on the magnitude of the load applied.

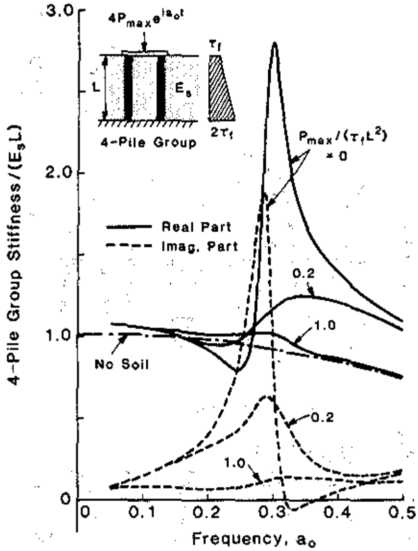

FIG. 10.—Pile-Head Stiffness of Pile Group

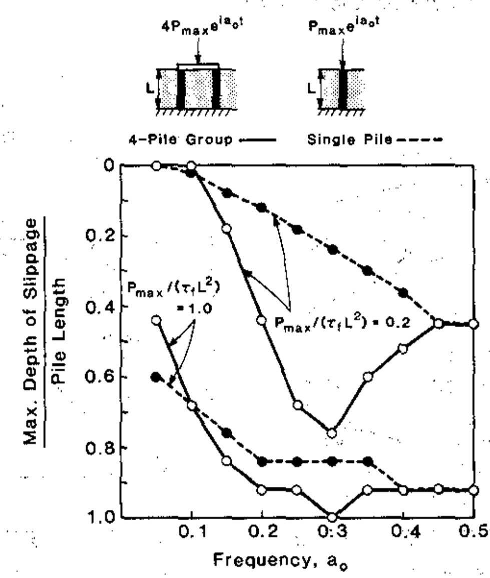

FIG. 11.—Maximum Depth of Slippage under Time Harmonic Excitation

2. For relatively small load level, the residual skin friction force pulls down the upper portion of pile but pulls up the lower portion of the pile.

3. For relatively large load level, the skin friction force pulls down the pile along the entire length.

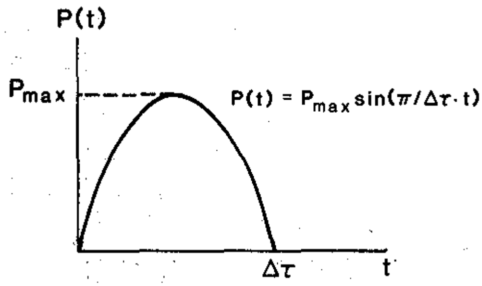

FIG. 12.—Transient Load Applied

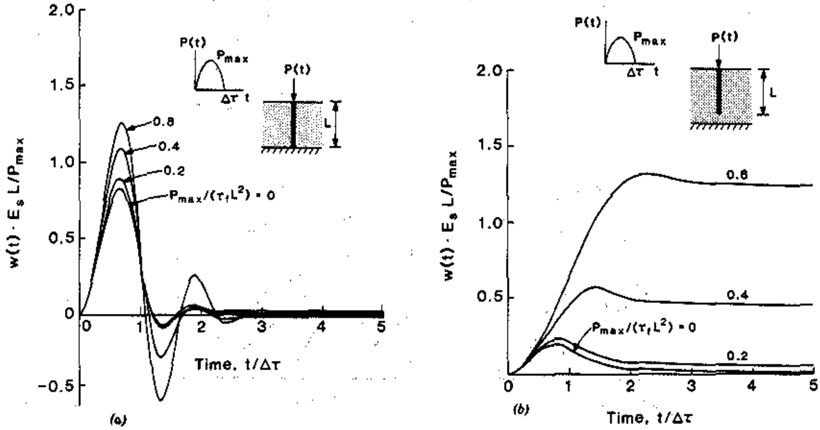

FIG. 13.—Time History of Pile-Head Displacement Due to Transient Load: (*a*) End-Bearing Pile; (*b*) Floating Pile

4. Because of the difference in skin friction distribution stated in 2 and 3, the maximum residual compression force is induced somewhere between the head and tip of the pile for relatively small load, whereas it is at the pile tip for relatively large load.

The energy dissipation due to radiation damping can be computed as

$$e_r = \int_0^t \int_0^L 2\pi r_0 \tau (\dot{W} - \dot{y}) dz dt \qquad (17)$$

where τ = skin friction stress at the side of the pile shaft. Fig. 15 shows the variation of the cumulative energy loss due to the radiation damping with time as a percentage of the total work applied to the floating pile considered. The percentages in the figure illustrate the degree of importance of the radiation damping in the nonlinear environments: the higher the percentage, more important the radiation damping is. As it is seen in the figure, the importance of the radiation decreases dramatically when the nonlinearity develops.

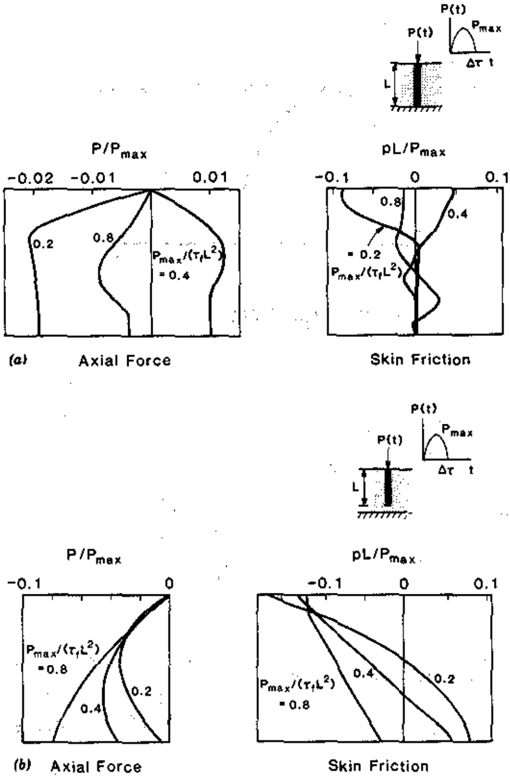

FIG. 14.—Residual Axial Shaft Force and Skin Friction after Application of Transient Load: (*a*) End-Bearing Pile; (*b*) Floating Pile

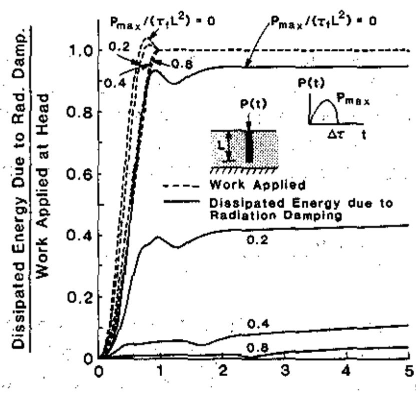

FIG. 15.—Variation of Cumulative Energy Loss Due to Radiation Damping

Conclusions

The nonlinearity of the soil-pile system is introduced in the previously formulated time domain formulation of dynamic responses of pile groups. It is assumed that the nonlinarity of the system is caused by slippage between the soil and pile at the soil-pile interface. The dynamic responses of nonlinear pile foundations are computed in order to demonstrate the present approach and to review briefly the effects of the nonlinearity on the dynamic response of pile foundations. Both harmonic and transient load are considered for this computation. The following are observed in the computed results:

1. Both the real and imaginary parts of the stiffness of single piles are reduced by the nonlinearity.
2. The nonlinearity tends to kill the wave interference effects and thus makes the stiffness markedly less dependent on the frequency compared with the case in which the nonlinearity is not considered.
3. The responses of floating and end-bearing piles to the transient load are markedly different when the piles are rather stiff.
4. The nonlinear conditions produce residual skin friction and residual axial force in the pile shaft.
5. The distribution pattern of the residual forces induced by the transient load are dependent on the magnitude of the load.

Acknowledgment

This work has been supported by the National Science Foundation under Grant No. CEE-8310623, of which K. Thirumalai is the NSF-program official. This support is gratefully acknowledged.

Appendix.—References

1. Angelides, D. C., and Roesset, J. M., "Nonlinear Dynamic Stiffness of Piles," *Research Report R80-13*, Department of Civil Engineering, M.I.T., Cambridge, Mass., 1980.
2. Blaney, G. W., Kausel, E., and Roesset, J. M., "Dynamic Stiffness of Piles," *Proceedings*, 2nd International Conference on Numerical Methods in Geomechanics, Blarkburg, Va., 1975.
3. Hardin, B. O., and Drnevich, V. P., "Shear Modulus and Damping in Soils: Design Equations and Curves," *Journal of the Soil Mechanics and Foundations Division*, ASCE, Vol. 98, No. SM7, July, 1972, pp. 667–692.
4. Kaynia, A. M., and Kausel, E., "Dynamic Stiffness and Seismic Response of Pile Groups," *Proceedings*, 2nd International Conference on Numerical Methods in Offshore Piling, I.C.E., Austin, Tex., 1982.
5. Konagai, K., and Nogami, T., "Time-Domain Axial Response of Dynamically Loaded Pile Groups," *Journal of Engineering Mechanics*, ASCE, Vol. 113, No. EM3, Mar., 1987.
6. Kuhlemeyer, R. L., "Vertical Vibration of Piles," *Journal of the Geotechnical Engineering Division*, ASCE, Vol. 105, No. GT2, Feb., 1979.
7. Kuhlemeyer, R. L., "Static and Dynamic Laterally Loaded Floating Piles," *Journal of the Geotechnical Engineering Division*, ASCE, Vol. 105, No. GT2, Feb., 1979, pp. 289–304.

8. Nogami, T., and Novak, M., "Soil-Pile Interaction in Vertical Vibration," *International Journal of Earthquake Engineering and Structural Dynamics*, Vol. 4, No. 3, 1976.
9. Nogami, T., and Novak, M., "Resistance of Soil to Horizontally Vibrating Pile," *International Journal of Earthquake Engineering and Structural Dynamics*, Vol. 5, No. 3, 1977.
10. Nogami, T., "Dynamic Group Effect of Multiple Piles Under Vertical Vibration," *Proceedings*, 3rd ASCE Engineering Mechanics Specialty Conference, Austin, Tex., 1979.
11. Nogami, T., "Dynamic Stiffness and Damping of Pile Groups in Inhomogeneous Soil," *ASCE Special Technical Publication on Dynamic Response of Pile Foundations: Analytical Aspect*, 1980, pp. 31–52.
12. Nogami, T., and Novak, M., "Coefficient of Soil Reaction to Pile Vibration," *Journal of the Geotechnical Engineering Division*, Vol. 106, No. GT5, May, 1980, pp. 565–570.
13. Nogami, T., "Dynamic Group Effect in Axial Response of Grouped Piles," *Journal of Geotechnical Engineering*, ASCE, Vol. 109, No. GT2, Feb., 1983, pp. 228–243.
14. Nogami, T., and Chen, H. L., "Behavior of Pile Groups Subjected to Dynamic Loading," *Proceedings*, 11th Canadian Conference on Earthquake Engineering, Vancouver, British Columbia, Canada, 1983, pp. 413–423.
15. Nogami, T., "Flexural Grouped Piles Under Dynamic Load," *International Journal of Earthquake Engineering and Structural Dynamics*, Vol. 13, No. 3, 1985, pp. 321–336.
16. Nogami, T., "Nonlinear Dynamic Winkler Model for Lateral Cyclic Response Analysis of Single Piles," *Proceedings*, 2nd International Conference on Soil Dynamics and Earthquake Engineering, held on the QEII, 1985, pp. 4.51–5.60.
17. Nogami, T., and Konagi, K., "Time Domain Axial Response of Dynamically Loaded Single Piles," *Journal of Engineering Mechanics*, ASCE, Vol. 112, No. EM11, Nov., 1986.
18. Novak, M., "Dynamic Stiffness and Damping of Piles," *Canadian Geotechnical Journal*, National Research Council of Canada, Vol. II, No. 4, 1974, pp. 574–598.
19. Novak, M., and Nogami, T., "Soil-Pile Interaction in Horizontal Vibration," *International Journal of Earthquake Engineering and Structural Dynamics*, Vol. 5, No. 3, 1977.
20. Sheta, M., and Novak, M., "Vertical Vibration of Pile Groups," *Journal of Geotechnical Engineering*, ASCE, Vol. 108, No. GT4, Apr., 1982.
21. Wass, G., and Hartman, H. G., "Analysis of Pile Foundations Under Dynamic Loads," SMIRT Conference, Paris, France, 1981.
22. Wolf, J. P., and Von Arx, G. A., "Impedance Function of Group of Vertical Piles," *Proceedings*, ASCE Specialty Conference on Soil Dynamics and Earthquake Engineering, Pasadena, Calif., 1978.